AIChE

Mechanistic Model for Kinetics of Propene Hydroformylation with Rh Catalyst

Dmitry Yu. Murzin, Andreas Bernas, and Tapio Salmi
Dept. of Chemical Engineering, Åbo Akademi University, Process Chemistry Centre, FI-20500 Åbo/Turku, Finland

DOI 10.1002/aic.12746
Published online September 12, 2011 in Wiley Online Library (wileyonlinelibrary.com).

Hydroformylation of propene to isobutyraldehyde and n-butyraldehyde was studied in the kinetic regime in a semibatch stainless steel reactor at 85–115∘C and 1–15 bar pressure in 2,2,4-trimethyl-1,3-pentanediol monoisobutyrate solvent with rhodium catalyst cyclohexyl diphenylphosphine as a ligand, which showed lower normal/isometric aldehyde ratio (n/i) than previously studied triphenylphosphine. The rate was pressure and Rh concentration dependent. The regioselectivity was conversion independent; however, dependent on the ligand concentration, as higher ligand concentration promoted isobutyraldehyde formation. The influence of ligand concentration on regioselectivity was investigated. A kinetic model was proposed based on the mechanism of alkene hydroformylation and compared with experimental observations. Numerical data fitting was performed showing good agreement of reaction rates and regioselectivity with experimental data. © 2011 American Institute of Chemical Engineers *AIChE J*, 58: 2192–2201, 2012
Keywords: hydroformylation, propene, rhodium, cyclohexyl diphenylphosphine, kinetic modeling

Introduction

Hydroformylation is the oldest and in production volume the largest homogeneously catalyzed industrial process. The hydroformylation reaction was discovered by Otto Roelen in 1938, and the reaction is also called oxosynthesis and Roelen's reaction.[1–4]

Hydroformylation of alkenes with carbon monoxide and hydrogen is a homogeneously catalyzed gas–liquid (G–L) reaction, which is used for the production of linear and branched aldehydes, as demonstrated in Figure 1.

A wide range of aldehydes having applications in perfumes, surfactants, plasticizers, and solvents is produced by this reaction, which is a typical case of simultaneous absorption of two or more gases, with reaction in a liquid medium or in an interfacial regime in the presence of a homogeneous catalyst.[5–12] The catalyst used in hydroformylation is typically an organometallic complex. Cobalt-based catalysts dominated hydroformylation until 1970s, after which rhodium-based catalysts were commercialized. The main part of the aldehydes formed is hydrogenated to alcohols or oxidized to carboxylic acids. Furthermore, the alcohols obtained can undergo further reactions, such as esterification. Thus, the aldehydes are typical intermediates for chemical industry.[13]

In recent years, a lot of effort has been put on the ligand chemistry, to find new ligands for tailored processes.[14,15] In spite of intensive research on hydroformylation in the last 50 years, both the reaction mechanisms and kinetics are not clear in most cases. Both associative and dissociative mechanisms have been proposed.[13,16] The discrepancies in mechanistic speculations have also lead to a variety of rate equations for hydroformylation processes. The concentrations of the reactant (substrate) alkene, the catalyst, as well as H_2 and CO are included in the kinetic expressions, but very little quantitative information on the effect of the ligands is available. Typically, the effects of the alkene, the catalyst, and H_2 are positive on the reaction kinetics, whereas an inhibitory effect of CO is characteristic for many rate equations proposed hitherto.[17] The general feature of previous studies has been that the partial pressures of H_2 and CO have not been screened systematically, thus the exact form of the rate equation remains obscured; for instance, the effect of CO cannot always be p_{CO}^{-1}, as proposed in some rate equations, but a zero-order or higher order behavior might become visible at lower CO pressures.[17]

A lot of research has been published on hydroformylation of alkenes, but the vast majority of the effort has been focused on the chemistry of various metal–ligand systems. In alkene hydroformylation with triphenylphosphine (TPP) ligand, the mechanism of hydrogen activation has been studied through *in situ* high-pressure Fourier transform infrared spectroscopy (FTIR).[18] NMR spectroscopy is also a useful tool for *in situ* studies.[19]

Quantitative kinetic studies including modeling of rates and selectivities, that is *n/i* ratio, are much scarcer. In this work, we present the approach to modeling of hydroformylation kinetics. Hydroformylation of propene with a rhodium-based catalyst was selected as a case study. The aim of this work is to discuss the mechanism of hydroformylation and to compare the kinetics, which corresponds to the mechanism, with experimental observations, focusing mainly on regioselectivity and using the theory of complex reactions.[20]

Experimental

In a typical experiment, the catalyst precursor (acetylacetonato)dicarbonylrhodium(I) (99%, Alfa Aesar) and the

Correspondence concerning this article should be addressed to D. Y. Murzin at dmurzin@abo.fi.

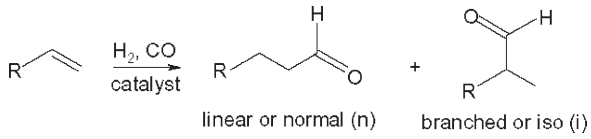

Figure 1. Scheme of alkene hydroformylation.

ligand cyclohexyl diphenylphosphine (CHDPP, PA, Acros Organics) were dissolved in 150 mL of 2,2,4-trimethyl-1,3-pentanediol monoisobutyrate or valeraldehyde (97%, Aldrich) in a vessel under nitrogen bubbling on a heating plate equipped with magnetic agitation at a temperature slightly less than the reaction temperature. After a period of 20–30 min, the ligand-modified complexes were formed as the solution turned into yellow-green color. All chemicals were nitrogen treated and stored under nitrogen to avoid any contact with air to prevent oxidation.

The experiments were carried out in a stirred and pressurized 300-mL Parr 4561 stainless steel reactor, which was designed to withstand a pressure of 300 bar at 350°C. It had an internal cooling loop and was equipped with an automatic temperature control system consisting of an external electric heating jacket coupled to a steering unit (Parr 4843), which was also used to control the stirring speed. The temperature could be maintained within ±1°C. The reactor had facilities for sampling of the liquid phase as well as the gaseous content, and it was connected to reservoirs of propene (99.5%, AGA) and nitrogen (99.999%, AGA). Synthesis gas containing a H_2/CO mixture of the composition 50.5 mol % CO and 49.5 mol % H_2 (99.995%, AGA) or 45.0 mol % CO and 55.0 mol % H_2 (99.995%, AGA) was fed at a constant pressure to the reactor with a pressure controller (Brooks 5866, Brooks 0154). The reactor was equipped with transducers for on-line measurements of temperature and pressure (Keller Type PA21 SR/80520.3-1), which was followed up on a PC for continuous data logging.

After charging the catalyst solution, the reactor was sealed tight and the heating jacket was attached. Gases fed into the reactor were dispersed in the liquid phase by the aid of a sinter filter for gas dispersion. Initially, the PC logging of temperature and pressure was started and the reactor was pressurized with 6 bar (overpressure) of nitrogen with all valves closed to check for leakage. Thereafter, the agitation was switched on at 1000 rpm and nitrogen was flushed through the reactor for 3 min at atmospheric pressure to remove any residues of oxygen before the experiment. The pressure was increased to 10 bar and kept at this level for 10 min. After reaching equilibrium between gas and liquid phases, the outlet was carefully opened. A propene volume of 2 L was flushed though the liquid phase with the flow 22 L/h for 7 min at 2.2 bar and ambient temperature. The reactor was kept closed for 25 min to await G–L equilibrium resulting in ~ 0.15 mol of propene in the liquid phase and thereafter heated to the reaction temperature while the pressure increased. After stabilization of the temperature, a zero sample was taken from the liquid phase. The stirring was kept on during this entire procedure.

The reaction time was initialized to zero as soon as the reactor was pressurized with hydrogen–carbon monoxide mixture. Samples of 1 mL were withdrawn from the liquid phase at certain time intervals. The weight was measured for all samples and the loss of the total liquid volume was taken into account in the calculations of the concentration profile. The temperature was slightly increasing in the beginning of the reaction. Typically, the conversion reached the value of 1 at 20–40 min; however, the total reaction time of 180 min was used to follow up possible changes after complete propene conversion.

As hydroformylation of propylene involves simultaneous dissolution and reaction of three gases in a liquid followed by a homogeneous catalytic reaction, it is important to ensure absence of mass-transfer limitations. In a separate study[21] that included experimental investigations and modeling, a reactor model was developed comprising both kinetics and mass transfer. The reactor content was described with a stirred tank model, that is the bulk phase has the same concentrations in the entire reaction volume. Consequently, the reactor consists of three regions: the gas phase, the liquid bulk phase, and the film region at the G–L interface. The chemical reactions take place in the bulk liquid and—eventually—also in the liquid film in the vicinity of the G–L interface. An even gas bubble-size distribution in the liquid phase was assumed. Because the reactor was operated in the semibatch mode, the fully dynamic model was used for the bulk phases and the liquid film.[21]

The model was able to predict under which circumstances the hydroformylation process is affected by liquid-phase diffusion of the reactants. The conclusion about hydroformylation was that the process easily becomes limited by the film diffusion and that intrinsic kinetics can be achieved under well-controlled laboratory conditions.

In this study, the experiments included in the kinetic model were carried out in the kinetic regime, which was confirmed by special experiments conducted at varied stirring rates.

Analyses of hydroformylation products for reaction follow-up were carried out by an internal standard method using a gas chromatographic technique for determination of isobutyraldehyde, *n*-butyraldehyde, propene, and propane in 2,2,4-trimethyl-1,3-pentanediol monoisobutyrate solvent. Because of propene and propane evaporation from the samples, the required initial amount of propene was calculated from the aldehyde products, as no side reactions were detected. A Hewlett Packard 5890 series II gas chromatograph with flame ionization detector operating at 300°C and split/splitless injector with HP GC Chem Station Rev. A.06.03 509 electronic integrator using a J&W Scientific DB-1 capillary column of the length 60 m and inner diameter 0.25 mm with 1-μm-film thickness was used. The injector operated in the split mode at 250°C and 1.93 bar, the oven temperature program was 30°C (0 min), 1°C/min:60°C (0 min), 15°C/min:300°C (40 min), and the gas flow rates of 3 mL/min carried gas helium, 28 mL/min make-up gas helium, 245 mL/min air, 41 mL/min hydrogen, and 202 mL/min split were applied.

Results and Discussion

Hydroformylation mechanism

The experimental observations collected previously for Rh/TPP and Ph/CHDPP[22] could be summarized as follows. The reaction orders in CO, propene, and hydrogen were equal to unity, whereas a negative order was obtained in the ligand concentration. Interestingly enough in Ref. 22, regioselectivity was seen to be independent on reactant concentrations, displaying weak dependence on the ligand concentration, in a way that higher ligand concentration promoted

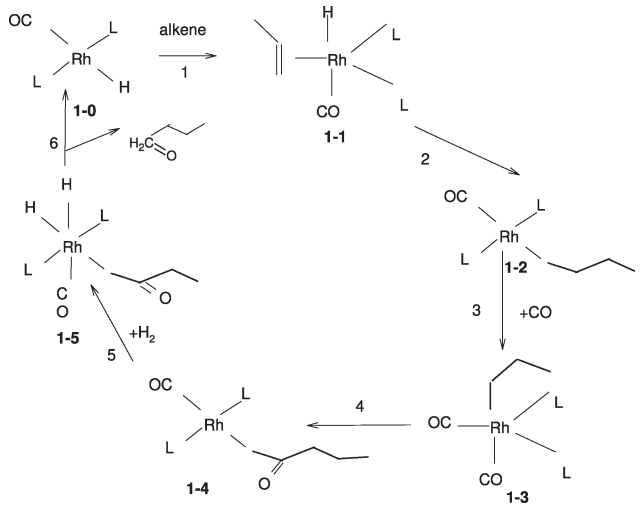

Figure 2. Selective hydroformylation of propene through $HRh(CO)(L)_2$ intermediate.

formation of the normal aldehyde. An attempt to model experimental data collected in Ref. 22 based on mechanistic ideas was made in Ref. 23. It is generally accepted that the active catalyst form is four coordinated intermediate $HRh(CO)(PPh_3)_2$ with two ligands, thus this intermediate was selected as the one giving selectively the normal aldehyde.[5–7] Monophosphine complexes were considered to be nonselective intermediates giving a mixture of linear and branched aldehydes. Even if the description of the data was fairly good, the model advanced in Ref. 23 contained some deficiencies. In particular, absence of any dependence of regioselectivity on CO concentration led to an exclusion of a step when four coordinated intermediate $HRh(CO)(PPh_3)_2$ leaves one ligand and accepts one CO molecule. Instead, formation of a RhHLCO complex with 14 electrons was proposed, which in fact should be rather unstable and is often considered as a precursor for complexes containing two Rh atoms. Moreover in Ref. 23, the catalytic cycles were somewhat simplified excluding several intermediates through lumping reaction steps. Finally, detailed chemistry of the four coordinated intermediate $HRh(CO)(PPh_3)_2$ reaction with the substrate giving two σ different alkyl intermediates leading respectively to normal and iso-aldehydes was not considered. In the present contribution, a set of data with CHDPP as the ligand was selected at different pressures of reactants having varying ligand concentrations with the aim to develop a kinetic model, which will be consistent not only with observed experimental data but also with the current views on hydroformylation mechanism.

Regioselectivity of the catalysts based on PPh_3 has been extensively studied in the literature,[3,5–7,24,25] and it was concluded that the number of phosphines coordinated to rhodium along with the stereochemistry at Rh determines the regioselectivity. The structures of the rhodium complexes that are present in the catalytic system were deduced by IR and NMR spectroscopy.[18,19,26,27] The relative concentration of four coordinated diphosphine $HRh(CO)(L)_2$ and monophosphine $HRh(CO)_2L$ are controlled by ligand and CO concentrations. It is generally accepted that during hydroformylation,[5–7,28] a large number of four and five coordinated complexes are present in the reaction milieu, and among the former species, $HRh(CO)(L)_2$ is a selective complex, whereas $HRh(CO)_2L$ is a nonselective one.[28]

In this article, we have adopted these mechanistic views and transformed them into tractable rate expressions.

The selective cycle involving $HRh(CO)(L)_2$ species and being in line with reaction mechanism is given in Figure 2. The mechanism starts with addition of alkene to $HRh(CO)(L)_2$ denoted as **1-0** forming a π-alkene Complex **1-1** with 18 electrons, which is isomerized in a 16 electrons σ-Complex **1-2**. The later one reacts with CO forming an alkyl Complex **1-3**, which isomerized into a σ-acyl Complex **1-4**, followed by addition of hydrogen and final release of the normal aldehyde from Complex **1-5** with a return to the initial Complex **1-0**.

Kinetic modeling of just this one cycle is rather complicated especially when all the steps are considered to be reversible. A catalytic cycle with 6 reversible steps was discussed in Ref. 29 leading to a following rate expression

$$r = \frac{\omega_1\omega_2\omega_3\omega_4\omega_5\omega_6 - \omega_{-1}\omega_{-2}\omega_{-3}\omega_{-4}\omega_{-5}\omega_{-6}}{D'} C_{\text{cat}} \quad (1)$$

where r is the rate for propene hydroformylation according to the mechanism in Figure 2, while the denominator in Eq. 1 in its more general form should contain 36 terms. Simplification for the case when all the steps are irreversible gives

$$r = \frac{\omega_1\omega_2\omega_3\omega_4\omega_5\omega_6}{D''} C_{\text{cat}} \quad (2)$$

with

$$D'' = \omega_1\omega_2\omega_3\omega_4\omega_5 + \omega_1\omega_2\omega_3\omega_4\omega_6 + \omega_1\omega_2\omega_3\omega_5\omega_6 + \omega_1\omega_2\omega_4\omega_5\omega_6 + \omega_1\omega_3\omega_4\omega_5\omega_6 + \omega_2\omega_3\omega_4\omega_5\omega_6 \quad (3)$$

where ω_1, and so forth are called frequencies of steps,[20] for example rates of these steps divided by concentrations of intermediate complexes. For example, for Figure 2, $\omega_1 = k_1 P_{\text{alkene}}$, whereas $\omega_{-1} = k_{-1}$. If all steps are considered irreversible than the rate expression of a following type can be obtained in a straightforward way from Eqs. 2 and 3

$$r = \frac{\omega_1 C_{\text{cat}}}{\frac{\omega_1\omega_2\omega_3\omega_4\omega_5}{\omega_2\omega_3\omega_4\omega_5\omega_6} + \frac{\omega_1\omega_2\omega_3\omega_4\omega_6}{\omega_2\omega_3\omega_4\omega_5\omega_6} + \frac{\omega_1\omega_2\omega_3\omega_5\omega_6}{\omega_2\omega_3\omega_4\omega_5\omega_6} + \frac{\omega_1\omega_2\omega_4\omega_5\omega_6}{\omega_2\omega_3\omega_4\omega_5\omega_6} + \frac{\omega_1\omega_3\omega_4\omega_5\omega_6}{\omega_2\omega_3\omega_4\omega_5\omega_6} + \frac{\omega_2\omega_3\omega_4\omega_5\omega_6}{\omega_2\omega_3\omega_4\omega_5\omega_6}} \quad (4)$$

giving

$$r = \frac{\omega_1 C_{\text{cat}}}{\frac{\omega_1}{\omega_6} + \frac{\omega_1}{\omega_5} + \frac{\omega_1}{\omega_4} + \frac{\omega_1}{\omega_3} + \frac{\omega_1}{\omega_2} + 1} = \frac{k_1 P_{\text{alk}} C_{\text{cat}}}{1 + k_1 P_{\text{alk}}\left(\frac{1}{k_2} + \frac{1}{k_4} + \frac{1}{k_6} + \frac{1}{k_3 P_{\text{CO}}} + \frac{1}{k_5 P_{\text{H}_2}}\right)} \quad (5)$$

Analysis of Eq. 5 demonstrated that it does not lead to first-order in all reactants. To circumvent this discrepancy, it is required to suppose that Steps from 1 to 5 are quasi-equilibrated, whereas Step 6 is controlling the overall rate. Detailed derivation will be presented below.

In addition to the cycle, demonstrated in Figure 2, $HRh(CO)_2L$ (Complex **2-0**) should be involved in a cycle leading to aldehydes.

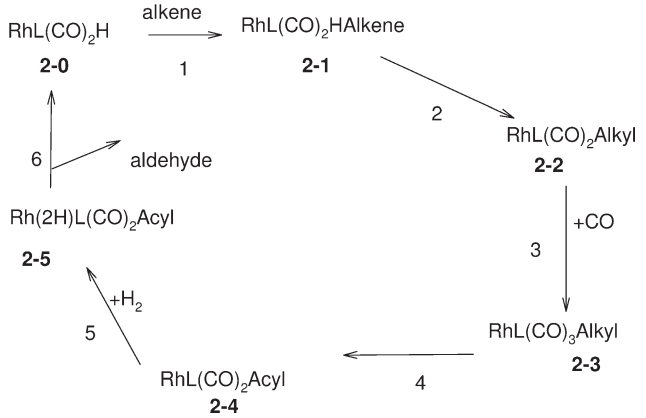

Figure 3. Hydroformylation of alkene through $HRh(CO)_2(L)$ intermediate.

Similar to the case of $HRh(CO)(L)_2$, intermediate Steps 1–5 will be considered quasi-equilibrated, whereas Step 6 is the rate-determining step. Following the original work of Wilkinson and coauthors,[26,27,30,31] hydroformylation through the cycle involving monophosphine intermediates given in Figure 3 was considered[5–7,28] not selective. Therefore in order to account for regioselectivity, two cycles involving two spatially different intermediates $HRh(CO)_2(L)$ should be proposed leading to either normal or iso-aldehyde. Such intermediates were discussed in the literature[5–7] and will be denoted here as $HRh(CO)_2(L)_{pro\text{-}iso}$ and $HRh(CO)_2(L)_{pro\text{-}normal}$. As already mentioned, the concept of one cycle very selective to normal aldehyde and two cycles leading to mixed aldehydes is required to explain regioselectivity dependence on the ligand concentration.

The link between two cycles can be envisaged in different ways. A simple interconversion (Figure 4a) will result in regioselectivity dependence on partial pressure of CO. In Refs. 5–7, such transformations were supposed to occur through species containing two CO and two phosphine species (Figure 4b) in the case of phosphine ligands.

It should be kept in mind that the catalyst precursor in this work was (acetylacetonato)dicarbonylrhodium(I), which reacts with the ligand forming first $HRh(CO)_2(L)$. This precursor is often used in hydroformylation reactions with different ligands and as aforementioned various spectroscopic data confirm that $Rh(acac)(CO)_2$ under the action of syngas turns into a coordinatively saturated hydride complex with the chelating ligand L ($HRh(CO)L_2$).[3,5–7,32,33] Logically, displacement of acetylacetonate by ligand occurs through formation of a monophosphine complex. As experimental procedure in this study was a typical one used in hydroformylation, it can be safely assumed that ($HRh(CO)L_2$) and ($HRh(CO)_2L$) were also synthesized in this work.

In order to explain dependence of regioselectivity only the ligand concentration, but not on the partial pressure of CO, in the current work a sequence of equilibria steps was proposed as demonstrated in Figure 5.

Species **4** are terminal ones, not leading to any reaction products. Finally, all these cycles can be combined together comprising an overall reaction graph. As one of the steps in Figure 5 is nonlinear, thus a simple two-dimensional (2-D) representation of the reaction graph is strictly speaking not possible, thus a somewhat simplified version is presented in Figure 6.

The reaction mechanism in Figure 6 can be utilized for derivation of the rate equations. To check the correctness of the reaction graph in Figure 6, an equation of Horiuti–Temkin[20] was used, which relates the number of basic routes, P (equal to three in the graph in Figure 6) with number of step S, the number of balance (or link) equations W, and the number of intermediates I, in a following way $P = S + W - I$. Balance (link) equations determine the relationship between intermediates. Such equations can correspond to the total concentration of intermediates equal to the initial catalyst concentration.

According to the rule of Horiuti–Temkin, the number of independent routes can be determined by subtracting from the number of steps, equal to 21 ($1'$ to $6'$, $1i$ to $6i$, $1n$ to $6n$, 7, 8, and 9), number of intermediates, equal to 20 (six in each of three cycles in addition to Complexes **3** and **4**) and adding the number of balance equations. One balance equation relates concentration of all rhodium containing intermediates. Following this rule it can be concluded that there should be another link equation, which must relate concentration of Species **4** with other reaction intermediates. It can be easily seen that as in Step 9 (Figure 6), equimolar amounts of **1-0** and **4** are produced, such balance equation links Species **4** with the sum of species of Type **1**.

$$C_4 = C_{1-0} + C_{1-1} + C_{1-2} + C_{1-3} + C_{1-4} + C_{1-5} + C_{1-6} \tag{6}$$

where C_4 is concentration of Complex **4**, and so forth.

Rate equations

Equilibria in the Route **I** of the reaction graph lead to the following equations for the concentrations of intermediate complexes

$$\begin{aligned} C_{2-1n} &= K_{1-n}P_pC_{2-0pro-n}, C_{2-2n} = K_{1-n}K_{2-n}P_pC_{2-0pro-n}, \\ C_{2-3n} &= K_{1-n}K_{2-n}K_{3-n}P_pP_{CO}C_{2-0pro-n} \\ C_{2-4n} &= K_{1-n}K_{2-n}K_{3-n}K_{4-n}P_pP_{CO}C_{2-0pro-n}, \\ C_{2-5n} &= K_{1-n}K_{2-n}K_{3-n}K_{4-n}K_{5-n}P_pP_{CO}P_{H_2}C_{2-0pro-n} \end{aligned} \tag{7}$$

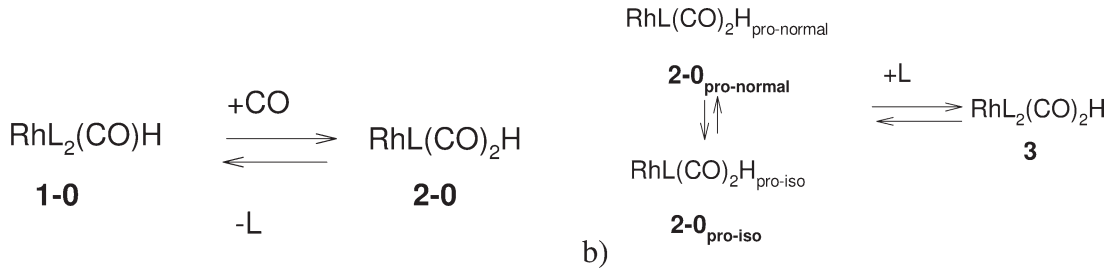

Figure 4. Interconversions between ligands (a) direct and (b) through $HRh(CO)_2(L)_2$.

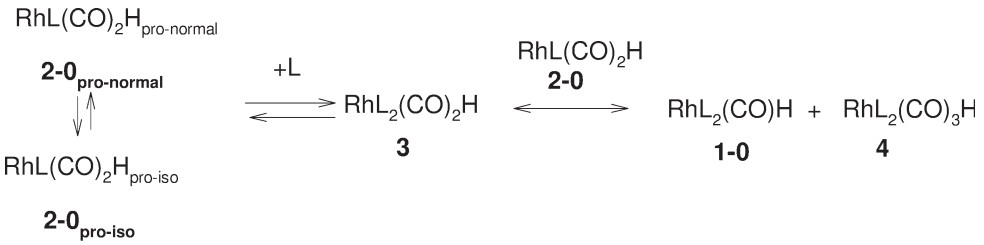

Figure 5. Interconversion between intermediates leading to linear and branched products.

Taking into account equilibria of Step 7

$$K_7 = \frac{C_{2-0\text{pro}-\text{iso}}}{C_{2-0\text{pro}-\text{n}}} \tag{8}$$

Concentrations of the intermediate complexes in the Route **II** could be written

$$\begin{aligned} C_{2-5i} = K_{1-i}K_7P_pC_{2-0\text{pro}-\text{n}}, C_{2-2i} = K_{1-i}K_{2-i}K_7P_pC_{2-0\text{pro}-\text{n}}, \\ C_{2-3i} = K_{1-i}K_{2-i}K_{3-i}K_7P_pP_{CO}C_{2-0\text{pro}-\text{n}}, \\ C_{2-4i} = K_{1-i}K_{2-i}K_{3-i}K_{4-i}K_7P_pP_{CO}C_{2-0\text{pro}-\text{n}}, \\ C_{2-5i} = K_{1-i}K_{2-i}K_{3-i}K_{4-i}K_{5-i}K_7P_pP_{CO}P_{H_2}C_{2-0\text{pro}-\text{n}} \end{aligned} \tag{9}$$

Equilibria 8 and 9 can be defined without distinction between **2-0** complexes

$$K_8 = \frac{C_3}{(C_{2-0\text{pro}-\text{n}} + C_{2-0\text{pro}-\text{iso}})C_L}; \quad K_9 = \frac{C_{1-0}C_4}{(C_{2-0\text{pro}-\text{n}} + C_{2-0\text{pro}-\text{iso}})C_3} \tag{10}$$

Similarly to the Routes **I** and **II** quasi-equilibria for the Route **III** result in

$$\begin{aligned} C_{1-1} = K_1'P_pC_{1-0}, C_{1-2} = K_1'K_2'P_pC_{1-0}, \\ C_{1-3} = K_1'K_2'K_3'P_pP_{CO}C_{1-0}, C_{1-4} = K_1'K_2'K_3'K_4'P_pP_{CO}C_{1-0}, \\ C_{1-5} = K_1'K_2'K_3'K_4'K_5'P_pP_{CO}P_{H_2}C_{1-0} \end{aligned} \tag{11}$$

From Eqs. 6, 10–12, one arrives at

$$C_3 = K_8(1 + K_7)C_{2-0\text{pro}-\text{n}}C_L \tag{12}$$

and

$$\begin{aligned} C_{1-0}^2(1 + K_1'P_p + K_1'K_2'P_p + K_1'K_2'K_3'P_pP_{CO} \\ + K_1'K_2'K_3'K_4'P_pP_{CO} + K_1'K_2'K_3'K_4'K_5'P_pP_{CO}P_{H_2}) \\ = K_9K_8(1 + K_7)^2C_{2-0\text{pro}-\text{n}}^2C_L \end{aligned} \tag{13}$$

As the reaction orders in propene, CO, and hydrogen are equal to unity, concentrations of Complexes **2-0** and **1-0** are larger than other concentrations in the respected cycles (routes), which means that in Eq. 13, for example unity is

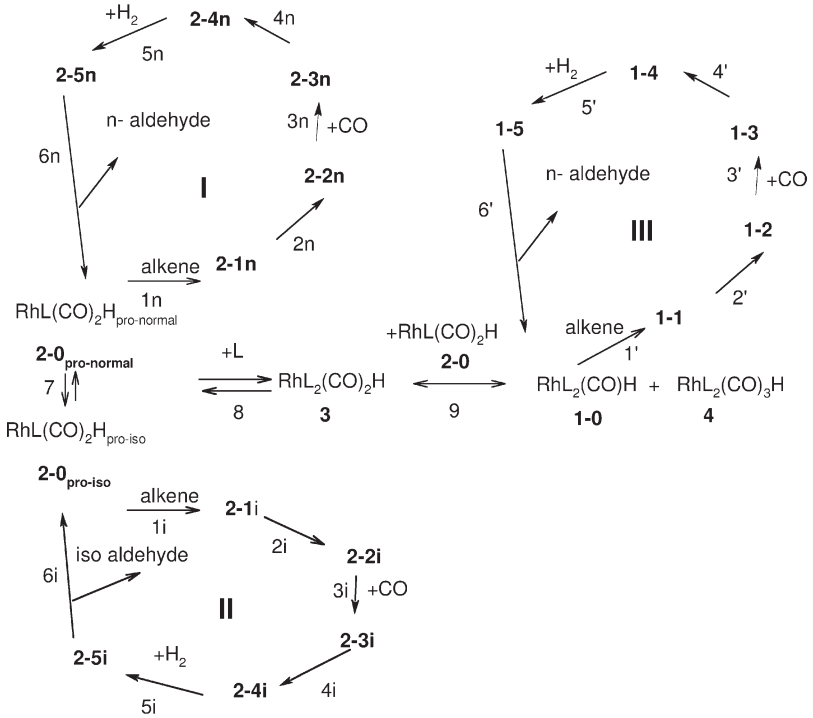

Figure 6. Reaction scheme of propene hydroformylation.

Table 1. Values of the Estimated Parameters for Rh/CHDPP Catalyst

Parameter	Estimated Value
A_a	0.618×10^{-3}
A_b	0.435×10^{-2}
C	0.188×10^{-1}
D	0.284×10^{-2}
A_e	0.300×10^{-2}
E_a	0.252×10^{5}

Dimensions: $[A_a]$ = min $(dm^3/mol)^3$; $[A_b]$ = min (dm^3/mol); $[c]$ = $(dm^3/mol)^{(1/2)}$; $[d]$ = dm^3/mol; $[A_e]$ = min $(dm^3/mol)^3$; and $[E_a]$ = kJ/mol. SRS = 0.2146×10^1 and $R^2 = 94.23\%$.

larger than other terms containing adsorption constants and partial pressures of reactants, leading to

$$C_{Rh} \approx C_{1-0} + C_{2-0pro-n} + C_{2-0pro-iso} + C_3 + C_4 \quad (14)$$

where

$$C_{1-0} \approx \sqrt{K_9 K_8 C_L}(1+K_7)C_{2-0pro-n}, C_4 \approx C_{1-0} \quad (15)$$

and thus

$$C_{2-0pro-n} = \frac{C_{Rh}}{1+K_7+2\sqrt{K_9K_8C_L}(1+K_7)+K_8(1+K_7)C_L} \quad (16)$$

The generation rate for the normal aldehyde, r_N is given by the relation

$$\begin{aligned} r_N &= k_{6n}C_{2-5n} + k'_6 C_{1-5} = \\ &= k_{6n}K_{1-n}K_{2-n}K_{3-n}K_{4-n}K_{5-n}P_pP_{CO}P_{H_2}C_{2-0pro-n} \\ &\quad + k'_6K'_1K'_2K'_3K'_4K'_5P_pP_{CO}P_{H_2}C_{1-0} \\ &= (k_{6n}K_{1-n}K_{2-n}K_{3-n}K_{4-n}K_{5-n}P_pP_{CO}P_{H_2} \\ &+ k'_6K'_1K'_2K'_3K'_4K'_5P_pP_{CO}P_{H_2}\sqrt{K_9K_8C_L}(1+K_7))C_{2-0pro-n} \\ &= (k_{6n}K_{1-n}K_{2-n}K_{3-n}K_{4-n}K_{5-n}P_pP_{CO}P_{H_2} \\ &\frac{+k'_6K'_1K'_2K'_3K'_4K'_5P_pP_{CO}P_{H_2}\sqrt{K_9K_8C_L}(1+K_7))}{1+K_7+2\sqrt{K_9K_8C_L}(1+K_7)+K_8(1+K_7)C_LC_{Rh}} \end{aligned} \quad (17)$$

Analogously for the isomeric aldehyde

$$\begin{aligned} r_I &= k_{6i}C_{2-5i} = k_{6i}K_{1-i}K_{2-i}K_{3-i}K_{4-i}K_{5-i}K_7P_pP_{CO}P_{H_2}C_{2-0pro-n} \\ &= \frac{k_{6i}K_{1-i}K_{2-i}K_{3-i}K_{4-i}K_{5-i}K_7P_pP_{CO}P_{H_2}}{1+K_7+2\sqrt{K_9K_8C_L}(1+K_7)+K_8(1+K_7)C_L}C_{Rh} \end{aligned} \quad (18)$$

Lumping constants together we get finally

$$r_N = \frac{(a+b\sqrt{C_L})P_pP_{CO}P_{H_2}}{1+c\sqrt{C_L}+dC_L}C_{Rh}, \quad r_I = \frac{eP_pP_{CO}P_{H_2}}{1+c\sqrt{C_L}+dC_L}C_{Rh} \quad (19)$$

With

$$\begin{aligned} &a = \frac{k_{6n}K_{1-n}K_{2-n}K_{3-n}K_{4-n}K_{5-n}}{1+K_7}; \quad b = \frac{k'_6K'_1K'_2K'_3K'_4K'_5\sqrt{K_9K_8}}{1+K_7}, \\ &c = 2\sqrt{K_9K_8}, d = K_8; \quad e = \frac{k_{6i}K_{1-i}K_{2-i}K_{3-i}K_{4-i}K_{5-i}K_7}{1+K_7} \end{aligned} \quad (20)$$

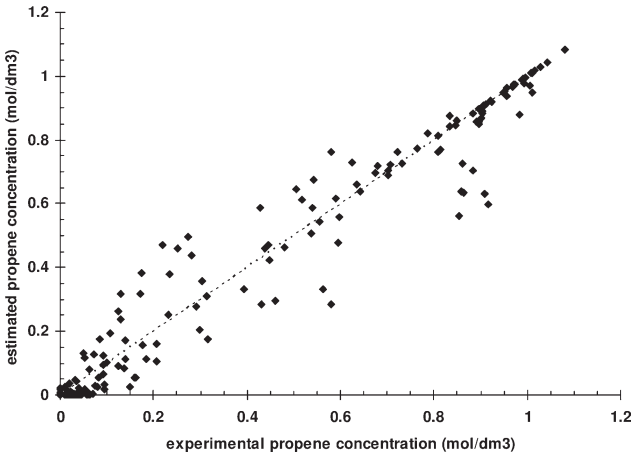

Figure 7. Parity diagram of the kinetic model in hydroformylation of propene with Rh/CHDPP catalysts.

As solubility data of H_2 and CO in the 2,2,4-trimethyl-1,3-pentanediol monoisobutyrate solvent are available,[34] the liquid-phase concentration of H_2 and CO was used instead of pressure. Similarly, the initial concentration of propene is calculated from the final product concentration. Thus, the rates become

$$r_N = \frac{(a+b\sqrt{C_L})C_pC_{CO}C_{H_2}}{1+c\sqrt{C_L}+dC_L}C_{Rh}, \quad r_I = \frac{eC_pC_{CO}C_{H_2}}{1+c\sqrt{C_L}+dC_L}C_{Rh} \quad (21)$$

where C_p (mol/dm^3), C_{H_2} (mol/dm^3), C_{CO} (mol/dm^3), C_{Rh} (mol/dm^3), and C_L (mol/dm^3) denote concentration of propene, hydrogen, carbon monoxide, rhodium, and ligand. The kinetic constants a, b, and e in Eq. 21 follow the Arrhenius dependence

$$\begin{aligned} a &= A_a \exp\left(\frac{-E_a}{R_{gas}}\left(\frac{1}{T}-\frac{1}{T_{mean}}\right)\right) \\ b &= A_b \exp\left(\frac{-E_a}{R_{gas}}\left(\frac{1}{T}-\frac{1}{T_{mean}}\right)\right) \\ e &= A_e \exp\left(\frac{-E_a}{R_{gas}}\left(\frac{1}{T}-\frac{1}{T_{mean}}\right)\right) \end{aligned} \quad (22)$$

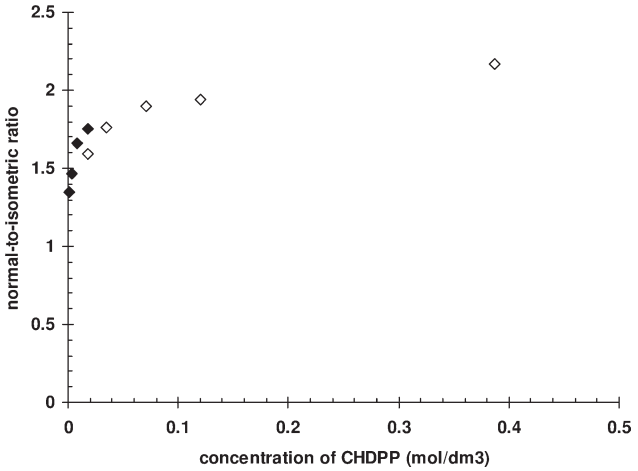

Figure 8. Normal-to-isometric ratio vs. ligand concentration.

Rhodium concentration: (◆) 0.000912 mol/dm^3, (◇) 0.00228 mol/dm^3.

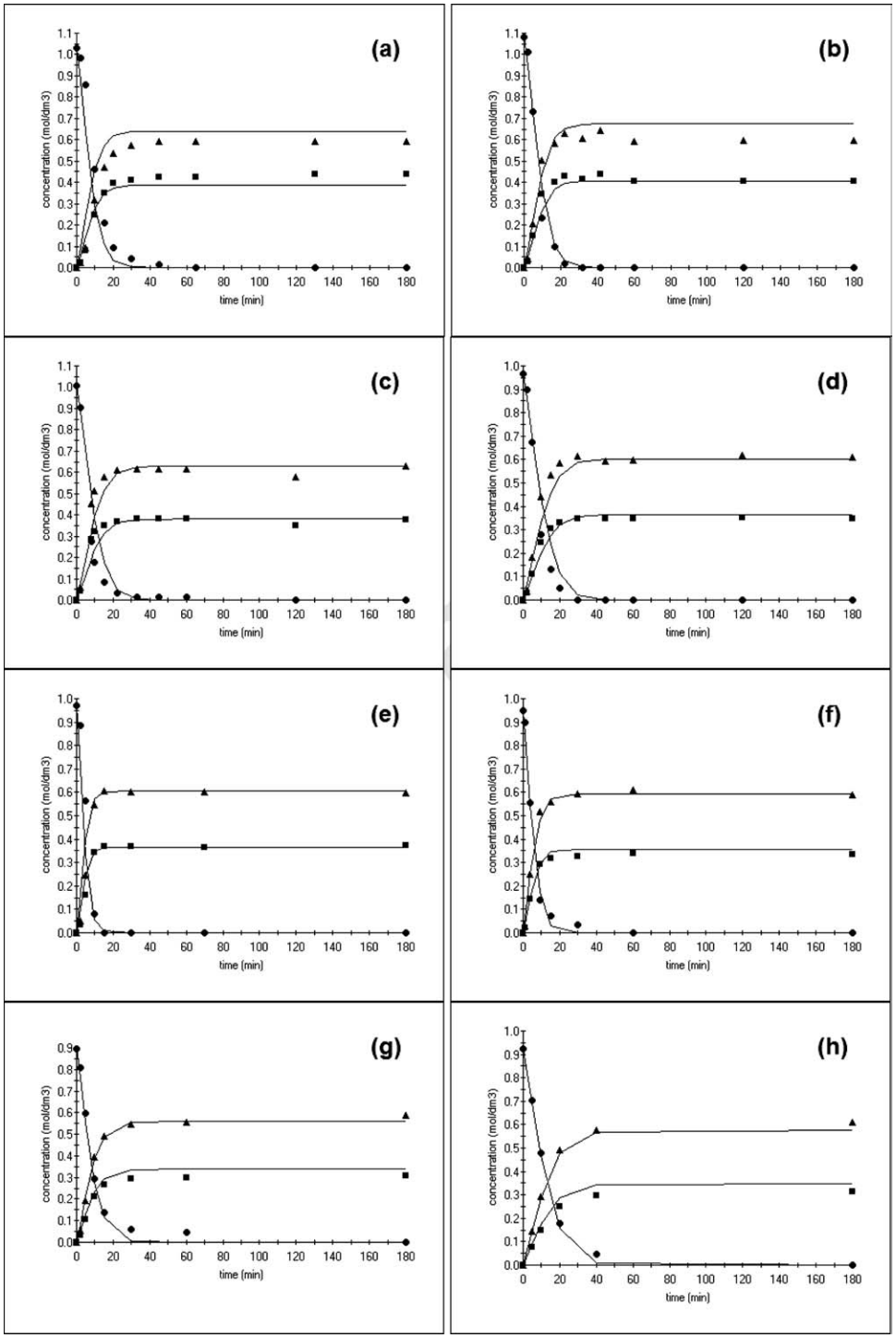

Figure 9. Comparison of predictions of the kinetic model (solid line) with experimental data (markers) for hydroformylation of propene with Rh/CHDPP catalyst.

(●) propene, (■) isobutyraldehyde, and (▲) *n*-butyraldehyde. Conditions: (a) $T = 100°C$, $p = 10$ bar, $C_{Rh} = 0.000912$ mol/dm^3, $C_L = 0.00087$ mol/dm^3, (b) $T = 100°C$, $p = 10$ bar, $C_{Rh} = 0.000912$ mol/dm^3, $C_L = 0.003483$ mol/dm^3, (c) $T = 100°C$, $p = 10$ bar, $C_{Rh} = 0.000912$ mol/dm^3, $C_L = 0.00872$ mol/dm^3, (d) $T = 100°C$, $p = 10$ bar, $C_{Rh} = 0.000912$ mol/dm^3, C_L=0.017484 mol/dm^3, (e) $T = 100°C$, $p = 10$ bar, $C_{Rh} = 0.00228$ mol/dm^3, $C_L = 0.017484$ mol/dm^3, (f) $T = 100°C$, $p = 10$ bar, $C_{Rh} = 0.00228$ mol/dm^3, $C_L = 0.035145$ mol/dm^3, (g) $T = 100°C$, $p = 10$ bar, $C_{Rh} = 0.00228$ mol/dm^3, $C_L = 0.071006$ mol/dm^3, (h) $T = 100°C$, $p = 10$ bar, $C_{Rh} = 0.00228$ mol/dm^3, C_L=0.120225 mol/dm^3, (i) $T = 100°C$, $p = 10$ bar, $C_{Rh} = 0.000456$ mol/dm^3, C_L=0.071006 mol/dm^3, (j) $T = 100°C$, $p = 10$ bar, $C_{Rh} = 0.000684$ mol/dm^3, C_L=0.071006 mol/dm^3, (k) $T = 100°C$, $p = 10$ bar, $C_{Rh} = 0.000912$ mol/dm^3, $C_L = 0.071006$ mol/dm^3, (l) $T = 85°C$, $p = 10$ bar, $C_{Rh} = 0.000912$ mol/dm^3, $C_L = 0.017484$ mol/dm^3, (m) $T = 115°C$, $p = 10$ bar, $C_{Rh} = 0.000912$ mol/dm^3, $C_L = 0.017484$ mol/dm^3, (n) $T = 100°C$, $p = 12$ bar, $C_{Rh} = 0.000912$ mol/dm^3, $C_L = 0.071006$ mol/dm^3, (o) $T = 100°C$, $p = 15$ bar, $C_{Rh} = 0.000912$ mol/dm^3, $C_L = 0.071006$ mol/dm^3.

In the expression above, A_a, A_b, A_e, E_a, R_{gas}, T, and T_{mean} denote frequency factor, activation energy, the gas constant, reaction temperature, and mean temperature of the experiments. The parameters a, b, and e in Eq. 21 have the same activation energy E_a, as the selectivity is not dependent on temperature. The constants to be estimated by regression

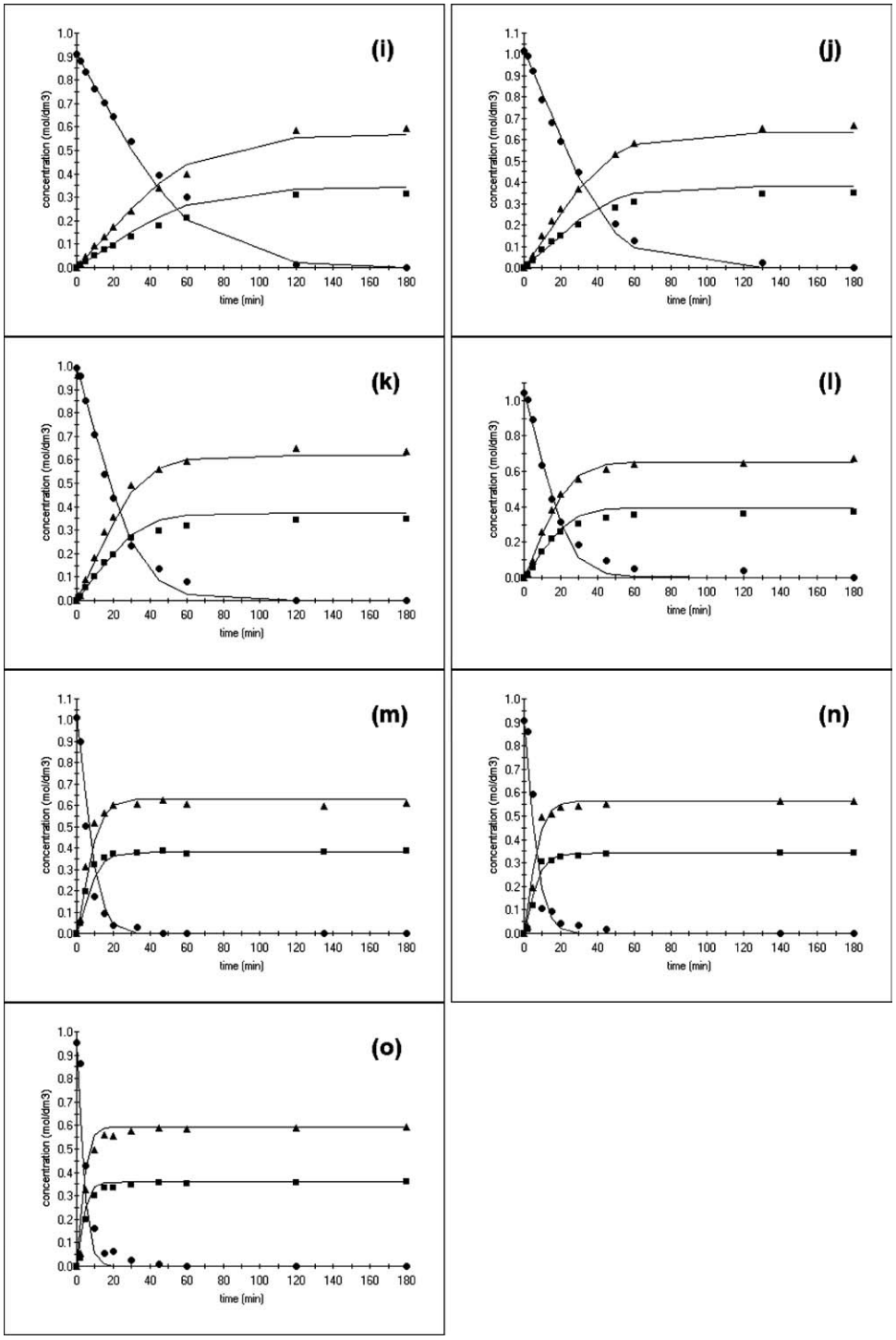

Figure 9. Continued

analysis are frequency factors and activation energy for the kinetic constants a, b, and e in Eq. 21 (hereafter referred to as A_a, A_b, A_e) as well as constants c and d in Eq. 21. The solubility of H_2 and CO in 2,2,4-trimethyl-1,3-pentanediol monoisobutyrate solvent follows the dependence

$$\ln\left(x_g\right) = A + \frac{B}{(T/K)} + C\ln(T/K) \tag{23}$$

where A, B, and C are 10.972, −1466.01, and −2.3931 as well as 17.413, −1398.4, and −3.419 for H_2 and CO, correspondingly. The pressure dependence of the gas solubility is at low-solubility and moderate pressure given by Henry's law. The total concentration of the liquid phase was calculated to 5.315 mol/dm^3 and the concentrations of H_2 and CO in the liquid phase are obtained by multiplication of solubility with total concentration.

The sum of generation rates of the reaction products *n*-butyraldehyde and isobutyraldehyde denoted by r_N and r_I, respectively, is equal to the consumption rate of propene

$$-\frac{dC_P}{dt} = \frac{dC_N}{dt} + \frac{dC_I}{dt} = r_N + r_I \tag{24}$$

C_N and C_I are concentrations of linear and branched aldehydes.

A non-negligible amount of propene, a volatile component, is present in the gas phase, thus a failure to account for it will lead to serious errors in the quality of the data obtained as well as in the values of CO and H_2 partial pressures used in rate analysis. The initial propene concentration, that is the number of total moles of propene per reactor volume, is the sum of the asymptotic concentrations of the products. The initial molar amount of propene in the gas phase was calculated from the ideal gas law. The G–L equilibrium was calculated from the number of total moles of propene per reactor volume and the molar number of propene in the gas phase. The liquid-phase concentration of propene, C_P in Eq. 24, is thus a function of the total propene amount obtained from the product concentrations according to the molar balance, which is decreasing with reaction time. Knowing the pressure of the synthesis gas fed into the reactor, G–L equilibrium and the partial pressure of propene, the partial pressures of CO and H_2 as a function of the reaction time are then easily calculated.

Calculations

The systems of differential Eq. 21 and 23 portraying the kinetic model was solved numerically in the parameter estimations with the backward difference method by minimization of the sum of residual squares, SRS, with non-linear regression analysis using the Simplex and Levenberg–Marquardt optimization algorithms implemented in the software Modest.[35] The sum of squares was minimized with respect to using a step size of 1×10^{-4} and a value of 1×10^{-18} for both the absolute and relative tolerances of the Simplex and Levenberg–Marquardt optimizer, starting with Simplex and thereafter switching to Levenberg–Marquardt.

Modeling results

The values of the estimated parameters of the kinetic model are presented in Table 1. Modeling of the hydroformylation with Rh/CHDPP catalyst resulted in SRS and R^2 values of SRS $= 0.2146 \times 10^{1}$ and $R^2 = 94.23\%$, correspondingly. The numerical solver proposes an activation energy of $E_a =$ 25.2 kJ/mol. The degree of explanation is larger than 0.9, although the number of parameters has been suppressed significantly. It can be concluded that the kinetic parameters are physically reasonable and in accordance with qualitative observations. A parity diagram of the model is presented in Figure 7. The model describes the observed concentrations well at all propene concentrations, although there are some random deviations. In the calculation procedure minima of the objective function were found for all the parameters.

The normal-to-isometric ratio as a function of CHDPP concentration is presented in Figure 8. The model predicts this dependence very well. Some selected graphs, presenting the data fitting between the kinetic model and the experimental points for the Rh/CHDPP catalyst, are illustrated in Figure 9. In all cases, a rather good agreement of the experiments with the model predictions can be observed. Increasing the CHDPP concentration resulted in lower overall reaction rate. At the same time the selectivity to isobutyraldehyde decreased, as seen in Figures 9a–d, e–h. Moreover, the rate increased with the Rh concentration, while the regioselectivity remained at a constant level, as shown in Figures 9i–k. The rate increases with temperature as shown in Figures 9l–m. Varying the pressure in Figures 9n–o did not influence the regioselectivity.

Finally, it can be noted that the earlier mechanism for alkene hydroformylation was proposed in accordance with literature data and experimental observations to account for kinetics of this reaction. The reaction network was supposed to contain multiple mechanistically different cycles, each of them giving linear or branched products. A complicated mechanism involving different intermediates was translated into tractable rate expressions. The general kinetic scheme was somewhat simplified while deriving kinetic equations by assuming one rate-determining step in each catalytic route, which was justified by the obtained kinetic regularities.

Conclusions

The kinetics of propene hydroformylation to isobutyraldehyde and *n*-butyraldehyde was studied in a semibatch stainless steel reactor over Rh/CHDPP catalyst using 2,2,4-trimethyl-1,3-pentanediol monoisobutyrate solvent. The influence of syngas pressure, rhodium concentration, and ligand concentration was investigated. The rate was pressure dependent, whereas Rh concentration showed first-order kinetic dependence. The regioselectivity was dependent on the ligand concentration. The *n*/*i* ratio vs. conversion always showed a linear dependence. The ligand concentration was the only variable affecting the *n*/*i* ratio. Rate increased and *n*/*i* ratio decreased when the ligand concentration was decreased. A mechanistic model was proposed based on the mechanism of alkene hydroformylation and compared with experimental observations. Numerical data fitting was performed showing good agreement of reaction rates and regioselectivity with experimental data. The experimental system was described as a perfectly mixed semibatch gas–liquid reactor. The concentrations of propene, isobutyraldehyde, *n*-butyraldehyde, carbon monoxide, and hydrogen were used in the parameter estimation. The kinetic model showed the R^2 value of more than 0.9, and it was possible to find minima of the objective function for the parameters. The model predicted the propene hydroformylation kinetic system very well.

Acknowledgments

This work is part of the activities at the Åbo Akademi Process Chemistry Centre within the Finnish Centre of Excellence Programme (2000–2011) by the Academy of Finland.

Notation

Rh/CHDPP = rhodium/cyclohexyl diphenylphosphine
n/*i* ratio = normal/isometric aldehyde ratio
rs = regioselectivity
$N(i)$ = independent basic route i
P = number of basic routes
S = number of stages
W = number of balance equations
I = number of intermediates
r = reaction rate
P = pressure
C = concentration
L = ligand
t = unit time
c_i = concentration of compound i
A = constant in gas solubility dependence
B = constant in gas solubility dependence
C = constant in gas solubility dependence
x = gas solubility
k = kinetic constant
a = kinetic constant [min$(dm^3/mol)^3$]
b = kinetic constant [min(dm^3/mol)]
c = kinetic constant [$(dm^3/mol)^{(1/2)}$]

d = kinetic constant [dm^3/mol]
e = kinetic constant [$min(dm^3/mol)^3$]
K = equilibrium constant
A = frequency factor
E_a = activation energy
R_{gas} = the gas constant
T = reaction temperature
T_{mean} = mean temperature of the experiments
SRS = sum of residual squares
R^2 = R-squared value

Literature Cited

1. Cornils B, Herrmann WA. Concepts in homogeneous catalysis: the industrial view. *J Catal*. 2003;216:23–31.
2. *The New Catalyst Technical Handbook*.Johnson Matthey, 2001.
3. Cornils B, Herrmann WA. In: Cornils B, Herrmann WA, editors. *Applied Homogeneous Catalysis with Organometallic Compounds: A Comprehensive Handbook in Three Volumes*.Weinheim: Wiley-VCH, 2002; Vol.1, *Chapter 1*.
4. Sheldon RA. *Chemicals from Synthesis Gas: Catalytic Reaction of CO and H_2*.Dordrecht: Reidel, 1983.
5. Van Leeuwen P, Claver C. *Rhodium Catalyzed Hydroformylation*. Dordrecht: Kluwer Academic Publishers, 2000.
6. Falbe J. *New Syntheses with Carbon Monoxide*. Berlin: Springer Verlag, 1980.
7. Torrent M, Sola M, Frenking G. Theoretical studies of some transition-metal-mediated reactions of industrial and synthetic importance. *Chem Rev*. 2000;100:439–493.
8. Beller M, Cornils B, Frohning CD, Kohlpaintner CW. Progress in hydroformylation and carbonylation. *J Mol Catal A*. 1995;104:17–85.
9. Heck RF. Synthesis and reactions of alkyl cobalt and acyl cobalt tetracarbonyls. *Adv Organomet Chem*. 1996;4:243–266.
10. Orchin M, Rupilius W. Mechanism of the oxo reaction. *Catal Rev*. 1972;6:85–131.
11. Suess-Fink G, Meister G. Transition metal clusters in homogeneous catalysis. *Adv Organomet Chem*. 1993;35:41–134.
12. Papadogianakis G, Sheldon RA. Catalytic conversions in water: environmentally attractive processes employing water soluble transition metal complexes. *New J Chem*. 1996;20:175–185.
13. Frohning CD, Kohlpaintner CW, Bohnen H. In: Cornils B, Herrmann WA, editors. *Applied Homogeneous Catalysis with Organometallic Compounds: A Comprehensive Handbook in Three Volumes*, 2nd ed. Weinheim: Wiley-VCH, 2002; Vol.1,*Chapter 2*.
14. Pruett RL, Smith JA. Low-pressure system for producing normal aldehydes by hydroformylation of α-olefins. *J Org Chem*. 1969;34:327–330.
15. Beller M, Cornils B, Frohning CD, Kohlpaintner CW. Progress in hydroformylation and carbonylation. *J Mol Catal A: Chem*. 1995;104:17–85.
16. Bohnen HW, Cornils B. Hydroformylation of alkenes: an industrial view of the status and importance. *Adv Catal*. 2002;47:1–64.
17. Chaudhari RV, Seayad A, Jayasree S. Kinetic modeling of homogeneous catalytic processes. *Catal Today*. 2001;66:371–380.
18. Caporali M, Frediani P, Salvini A, Laurenczy G. In situ high pressure FT-IR spectroscopy on alkene hydroformylation catalyzed by $RhH(CO)(PPh_3)_3$ and $Co_2(CO)_8$. *Inorg Chim Acta*. 2004;357:4537–4543.
19. Bianchini C, Lee HM, Meli A, Vizza F. In situ high-pressure $^{31}P\{^1H\}$ NMR studies of the hydroformylation of 1-hexene by $RhH(CO)(PPh_3)_3$. *Organometallics*. 2000;19:849–853.
20. Temkin MI. The kinetics of some industrial heterogeneous catalytic reactions. *Adv Catal*. 1979;28:173–281.
21. Bernas A, Wärnå J, Mäki-Arvela P, Murzin DY, Salmi T. Kinetics and mass transfer in hydroformylation—bulk or film reaction? *Can J Chem Eng*. 2010;88:618–624.
22. Bernas A, Mäki-Arvela P, Lehtonen J, Salmi T, Murzin DY. Kinetic modeling of propene hydroformylation with Rh/TPP and Rh/CHDPP catalysts. *Ind Eng Chem Res*. 2008;47:4317–4324.
23. Murzin DY, Bernas A, Salmi T. Kinetic modeling of regioselectivity in alkenes hydroformylation over rhodium. *J Mol Catal A: Chem*. 2010;215:148–154.
24. Pruett RL. Hydroformylation. *Adv Organomet Chem*. 1979;17:1–60.
25. Trzeciak AM, Ziolkowski JJ. Perspectives of rhodium organometallic catalysis. Fundamental and applied aspects of hydroformylation. *Coord Chem Rev*. 1999;190–192:883–900.
26. Yagupsky G, Brown CK, Wilkinson G. Intermediates or their analogues in hydroformylation of alkenes catalysed by hydridocarbonyltris-(triphenylphosphine)rhodium(I). *Chem Commun*. 1969;1244–1245.
27. Yagupsky G, Brown CK, Wilkinson G. Further studies on hydridocarbonyltris(triphenylphosphine)rhodium(I); intermediate species in hydroformylation; rhodium and iridium Analogues. *J Chem Soc A*. 1970;1392–1401.
28. Hartwig J. *Organotransition Metal Chemistry, from Bonding to Catalysis*. Sausalito, USA: University Science Books, 2010.
29. Murzin D, Salmi T. *Catalytic Kinetics*. Amsterdam: Elsevier, 2005.
30. Evans D, Osborn JA, Wilkonson G. Hydroformylation of alkenes by use of rhodium complex catalysts. *J Chem Soc A*. 1968;3131–3142.
31. Evans D, Yagupsky G, Wilkinson G. The reaction of hydridocarbonyltris-(triphenylphosphine)rhodium with carbon monoxide, and of the reaction products, hydridodicarbonylbis(triphenylphosphine)rhodium and dimeric species, with hydrogen, *J Chem Soc A*. 1968;2660–2665.
32. van Rooy A, Kamer PCJ, van Leeuwen PCJ, Goubitz K, Fraanje J, Veldman N, Spek AL. Bulky diphosphite-modified rhodium catalysts: hydroformylation and characterization. *Organometallics*. 1996;15:835–847.
33. Rush SN, Noskov YuG, Kron TE, Korneeva GA. Kinetics and mechanism of propene hydroformylation catalyzed by rhodium complexes with a diphosphite ligand. *Kinet Catal*. 2009;50:557–566.
34. Still C, Salmi T, Mäki-Arvela P, Eränen K, Murzin DY, Lehtonen J. Solubility of gases in a hydroformylation solvent. *Chem Eng Sci*. 2006;61:3698–3704.
35. Haario H. *Modest User's Guide*. Profmath Oy: Helsinki, 2001.

Manuscript received May 6, 2011, and revision received July 18, 2011.